ASME 2018 12th International Conference on Energy Sustainability
June 26th, 2018

SAND2022-5007C

ON-SUN TESTING OF A HIGH TEMPERATURE BLADED SOLAR RECEIVER AND TRANSIENT EFFICIENCY EVALUATION USING AIR

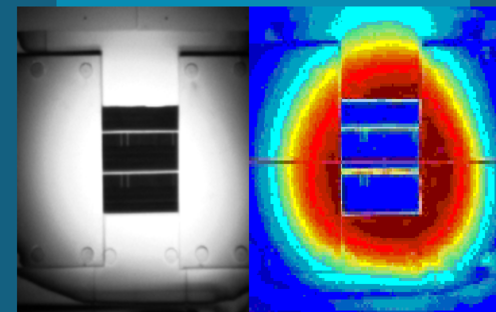

PowerEnergy2018-7543

Authors

Jesus Ortega, Sagar Khivsara, Joshua Christian, Pradip Dutta, and Clifford Ho

Agenda

1. Introduction
2. Experimental Details
3. Optical and CFD Modeling Details
4. Modified Efficiency Methodology
5. On-sun Testing Results
6. Conclusions and Future Steps

Introduction

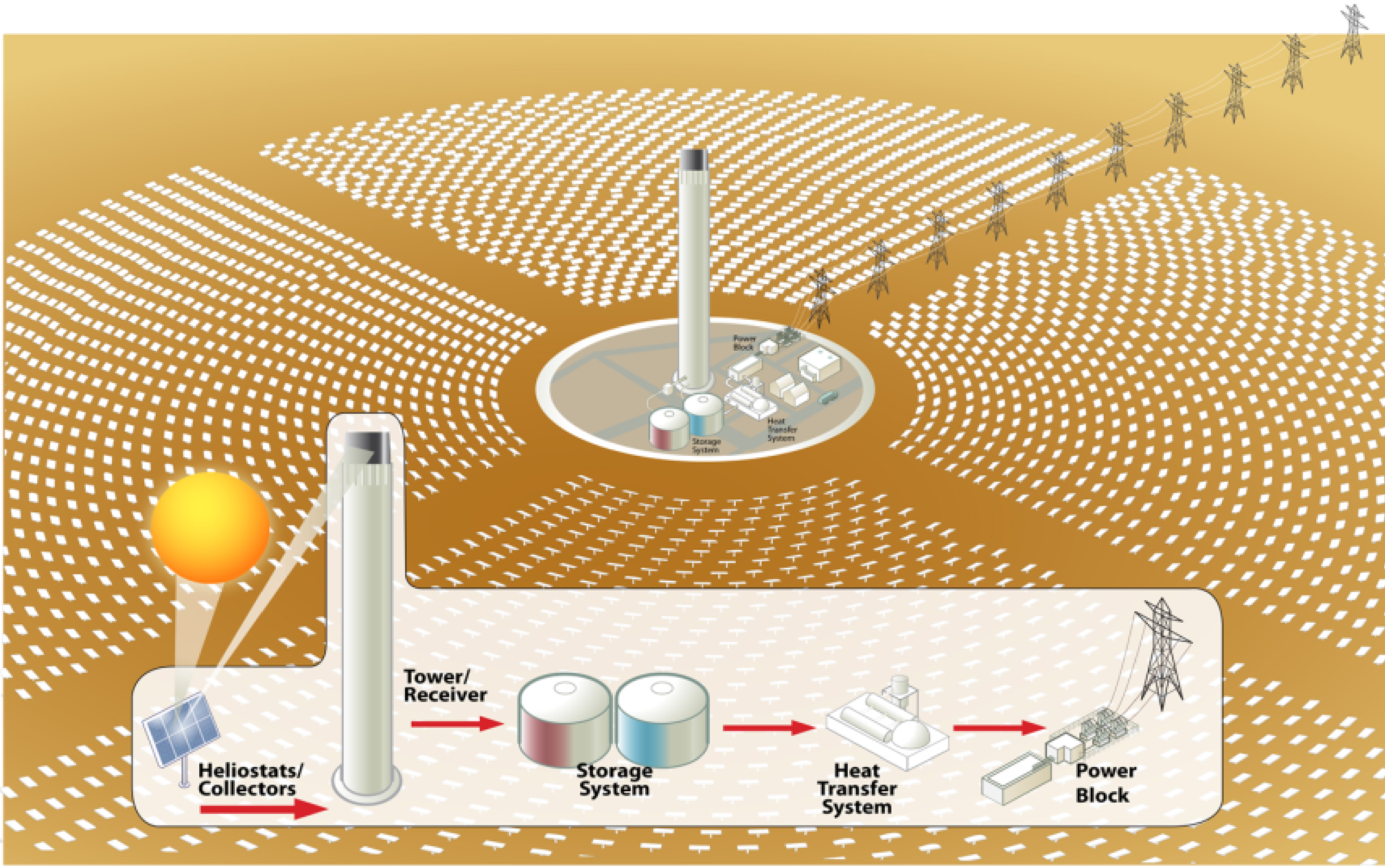

Introduction

- Concentrating solar receivers typically use coatings to enhance solar absorptance.
- Coatings degrade and need to be re-applied periodically, which affects performance and increases O&M cost.
- Conventional solar receivers are cylindrical or cubic.

Crescent Dunes Receiver

Ivanpah Receiver

Previous Work

- 2016: we completed the design and manufacturing of a Bladed Gas Tubular Receiver and we performed the first set of on-sun receiver tests using air from a compressor

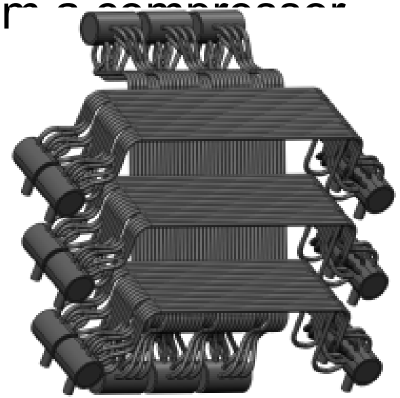

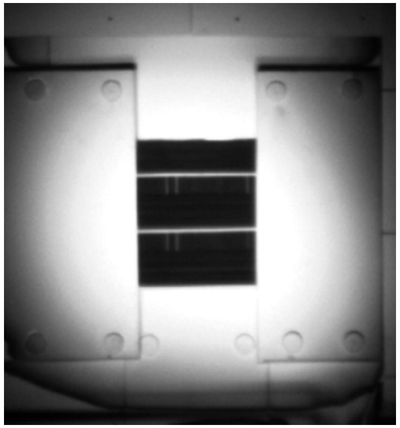

- Early 2017: we completed the design and assembly of a bottled gas test-loop to use with different gases

On-sun Test Details

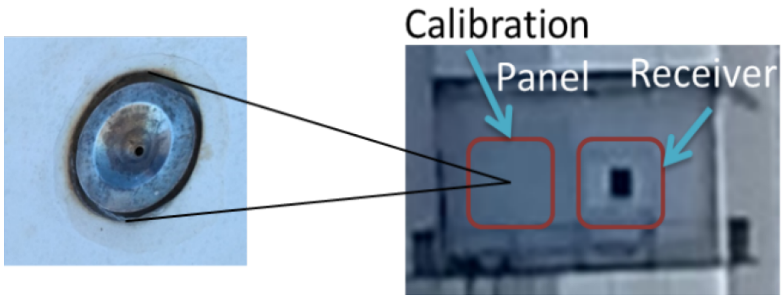

Radiometer for heat flux measurement

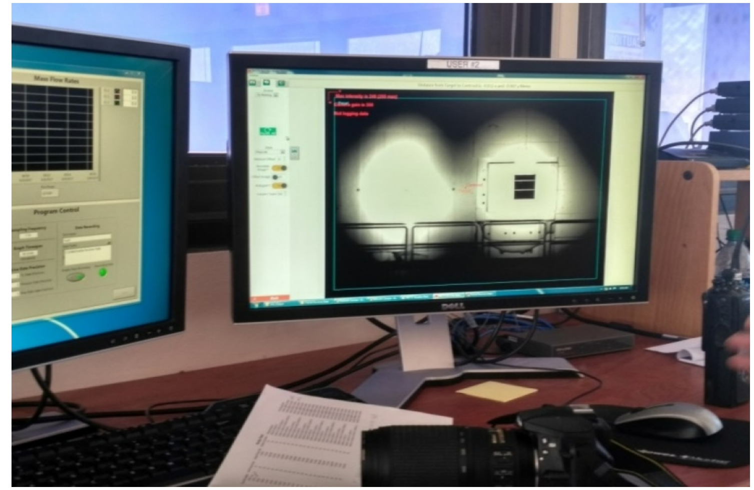

Imaging methods for flux characterization

Manifold regulator for gas supply

Pressurized gas supply (18 bottles)

On-sun test Procedure

- Initially, receiver is carefully preheated with no flow.
- The flow is enabled and the preheating flux is swapped for the test flux
- The on-sun test takes place for 12-15 minutes before the cool down

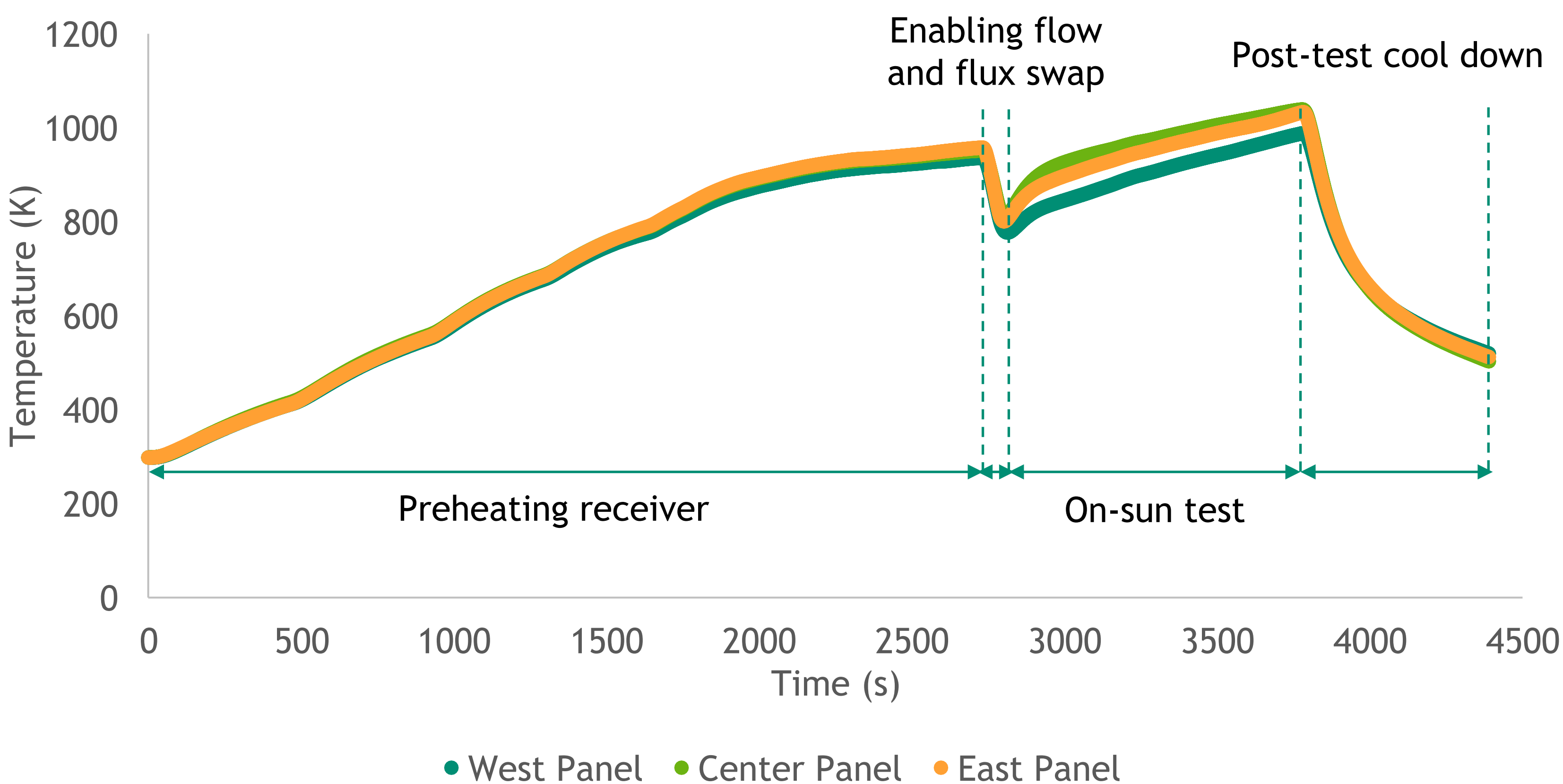

Optical and CFD Modeling Details

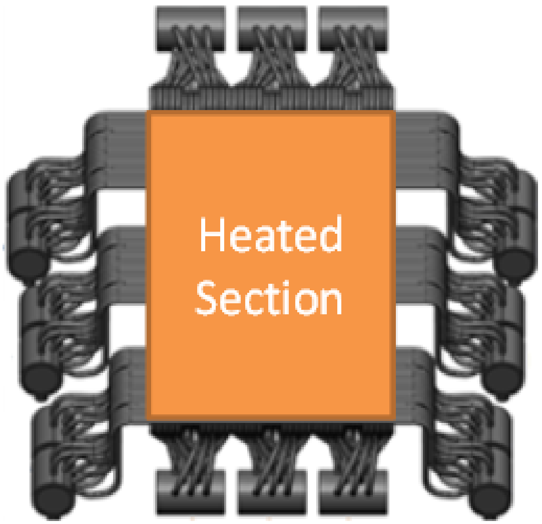

Insulated area is not directly heated

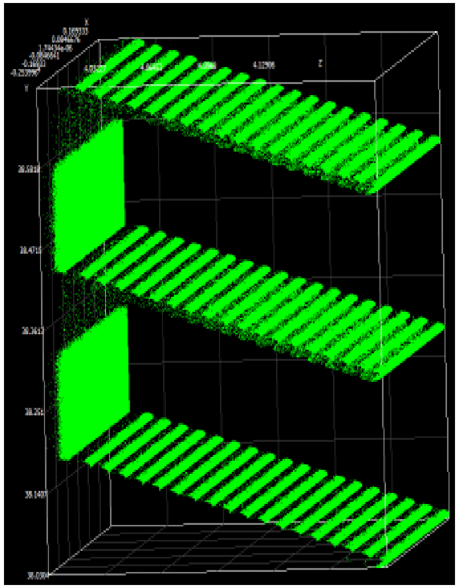

Ray tracing performed in SolTrace to produce heat flux profiles

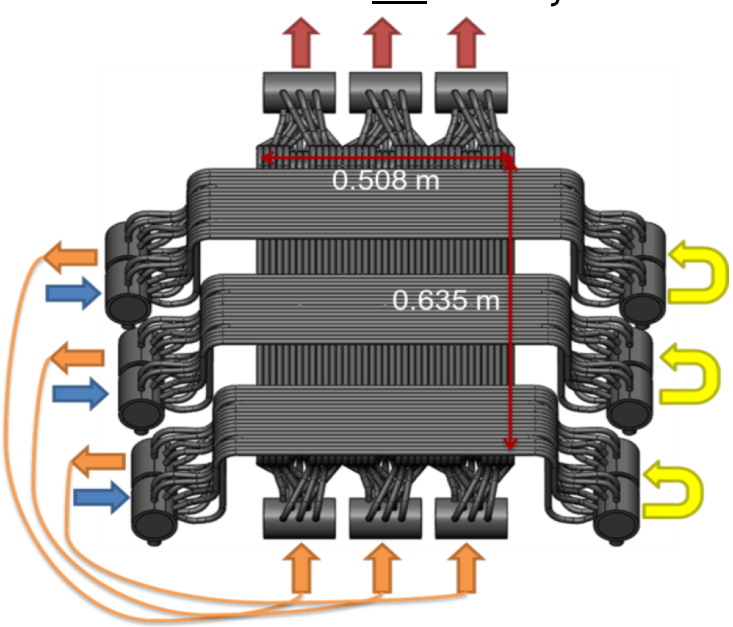

Flow path through the receiver

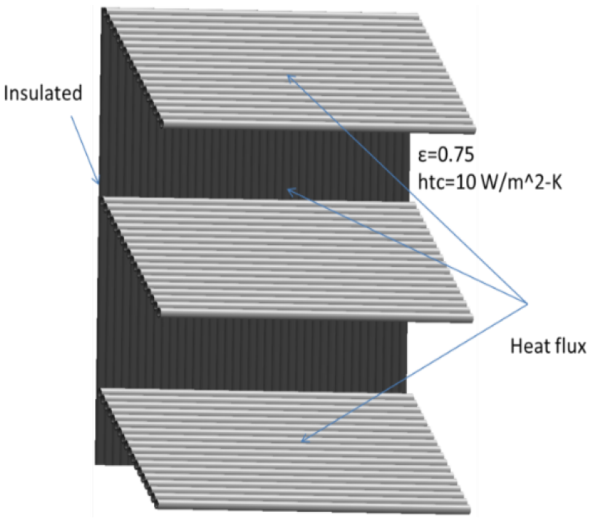

External boundary conditions in CFD model

Modified Efficiency Methodology

- For our receiver, the steady state efficiency can be calculated at any time by accounting for the heat absorbed by the gas as:

$$\varphi^k = \frac{\sum_{i=1}^{3} \dot{m}_i^k \int_{T_{in}^k}^{T_{out}^k} Cp_f(T)dT}{\dot{Q}_{incident}^k}$$

- However, the insulated sections of the receiver that are not directly heated and they absorb part of the heat absorbed by the fluid.
- To account for the heat absorbed by the insulated regions, we propose a modified efficiency calculation at every time-step that considers the isothermal temperature increase of these regions as part of the heat absorbed by the fluid.

$$T_j^k = T_j^{k-1} + \boxed{\frac{hA_s(T_f^k - T_j^{k-1})(t^k - t^{k-1})}{m_{h,j}Cp_h}}$$

Temperature increase due to heat transferred from fluid to insulated region

$$\dot{Q}^k{}_{total} = \sum_{i=1}^{3} \dot{m}_i^k \int_{T_{in}^k}^{T_{out}^k} Cp_f(T)dT + \boxed{\sum_{j=1}^{6} \frac{m_{h,j}Cp_h(T_j^k - T_j^{k-1})}{t^k - t^{k-1}}}$$

Heat transferred from fluid to insulated region

$$\varphi^k = \frac{\dot{Q}_{total}^k}{\dot{Q}_{incident}^k}$$

fied Efficiency Methodology

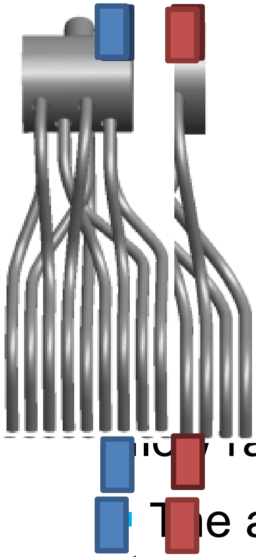

- count for the heat lost to the insulated sections, the heat transfer ient (HTC) was modeled as a function of temperature for a mass ate of 15 g/s.
- T e average HTC over the entire region was modeled across a range of temperatures and two flow directions for the two panel types.

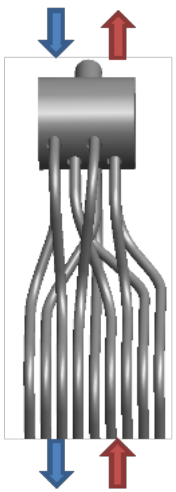

Fin panel headers and joints

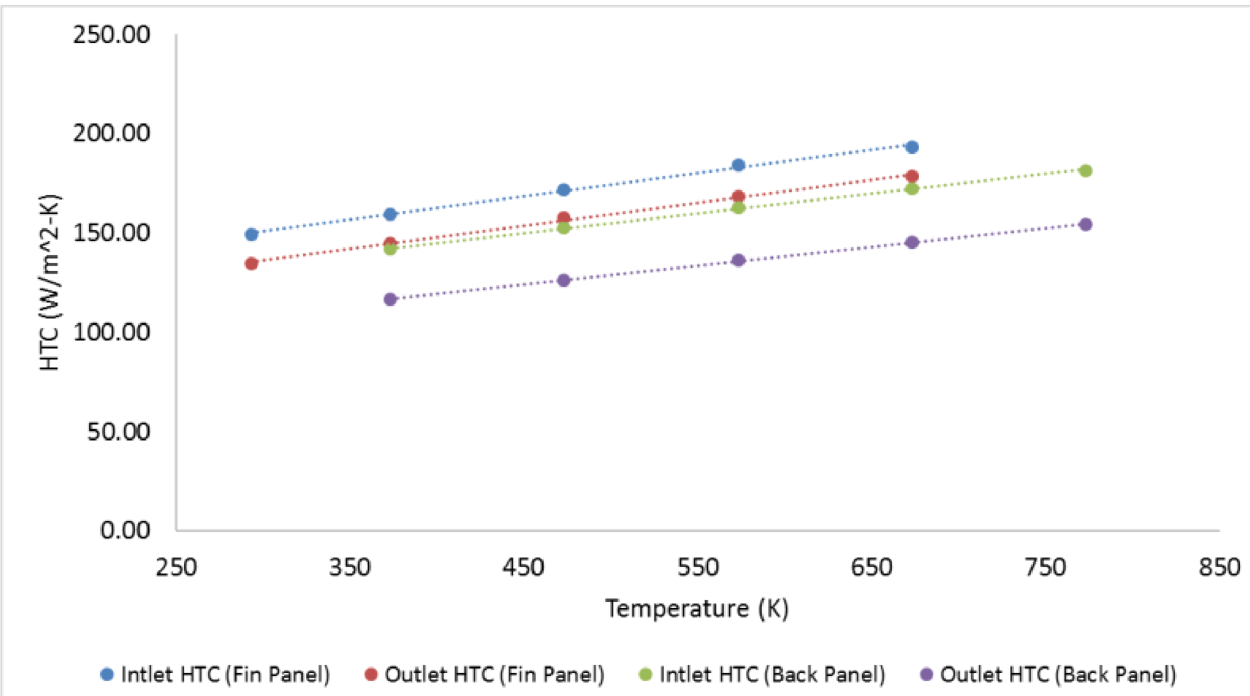

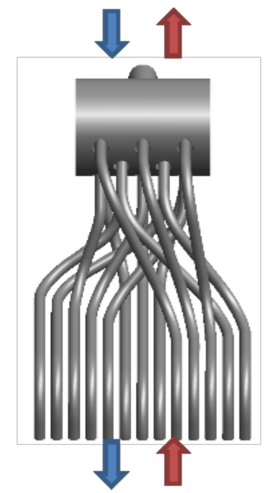

Back panel headers and joints

On-sun Testing Results

- The modified efficiency calculation proposed yields a receiver efficiency which is ~5% greater than the standard method.
- While the tests exhibit a highly transient behavior, this efficiencies are conservatively below the steady-state efficiency.

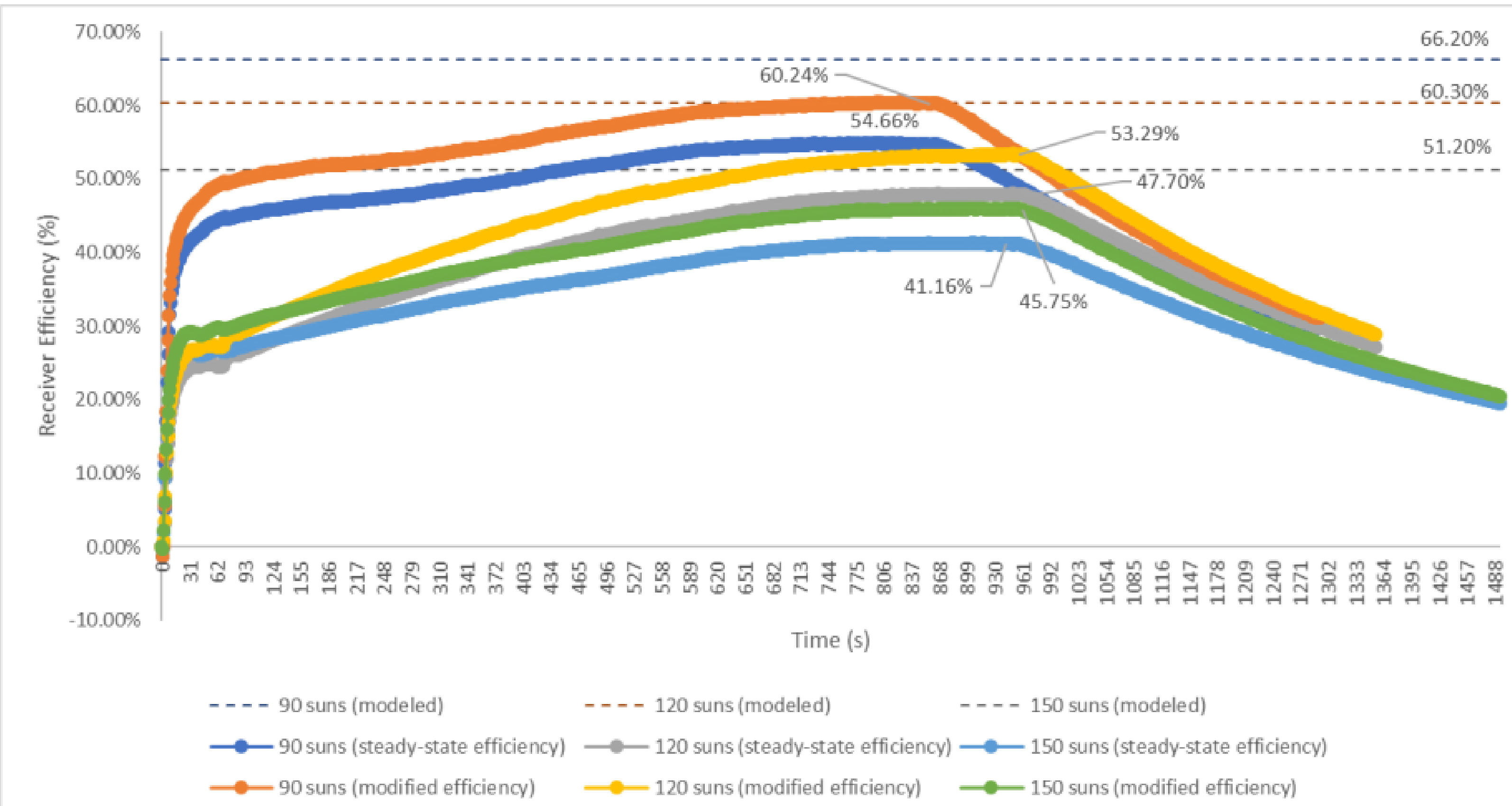

Conclusions and Future Steps

- A modified efficiency methodology to calculate the receiver efficiency by accounting for the transient nature and heat transfer to the header was presented.
- The bladed receiver was successfully demonstrated to deliver air at an outlet temperature up to 500 °C at an efficiency >50 % and the computational model limitations and similarities to the experiment were established in this work.
- The low thermal efficiency can be attributed to the low heat fluxes and the transient nature of the tests which do not achieve steady state operation.

- We have recently completed the on-sun evaluation of the bladed receiver using Nitrogen, Argon, and a Nitrogen-Argon mixture which shows efficiency increases of ~ 5-8% compared to Air.
- The scalability of these results to higher power levels will be analyzed in the upcoming work.

Acknowledgements

This research is based upon work supported by the Solar Energy Research Institute for India and the U.S. (SERIIUS) funded jointly by the U.S. Department of Energy subcontract DE AC36-08G028308 (Office of Science, Office of Basic Energy Sciences, and Energy Efficiency and Renewable Energy, Solar Energy Technology Program, with support from the Office of International Affairs) and the Government of India subcontract IUSSTF/JCERDC-SERIIUS/2012 dated 22nd Nov. 2012.

Jesus Ortega
jdorte@sandia.gov

Questions?

Back-up Slides

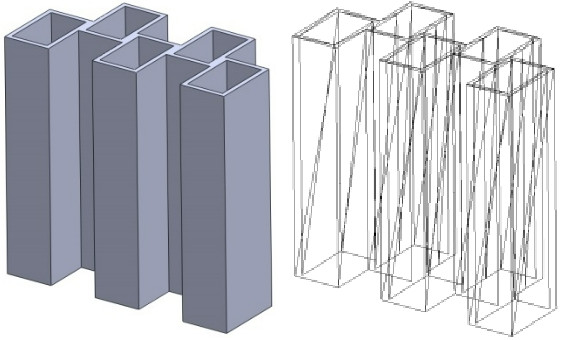

Save CAD geometry as an STL file.

↓

MATLAB: Pre-process STL file into a Stage file for SolTrace.

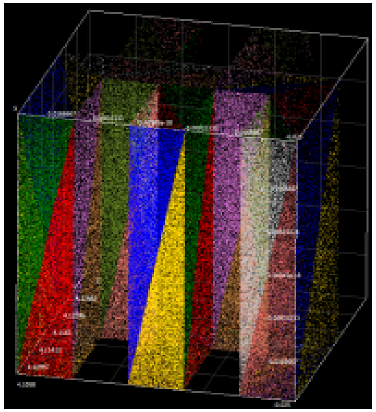

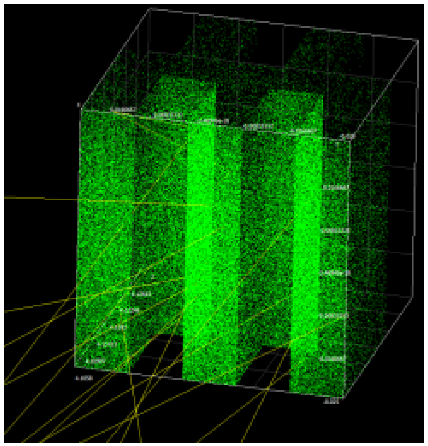

↓

SolTrace: Perform ray tracing using the heliostat field or solar furnace ideal models from NSTTF.

↓

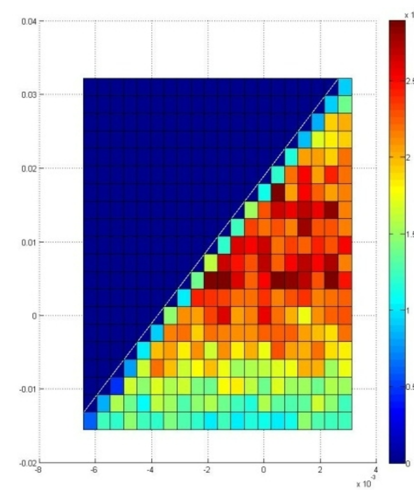

MATLAB: Post-process ray data file to create 2-D heat flux maps.

↓

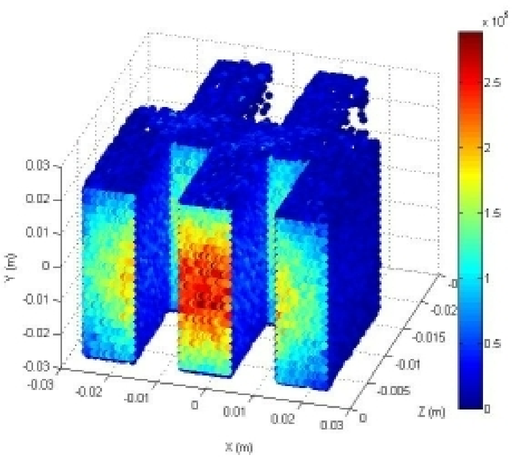

FLUENT: Heat flux profiles can be imported to be used as boundary conditions.

Pipe Design

- The tubes and inlet/outlet pipes were selected to be made out of ½" (12.7 mm O.D.) Inconel 625 tube and ¾" (1.05" or 26.67 mm O.D.) Inconel 625 pipe
- The same design conditions are used in the tube and pipe

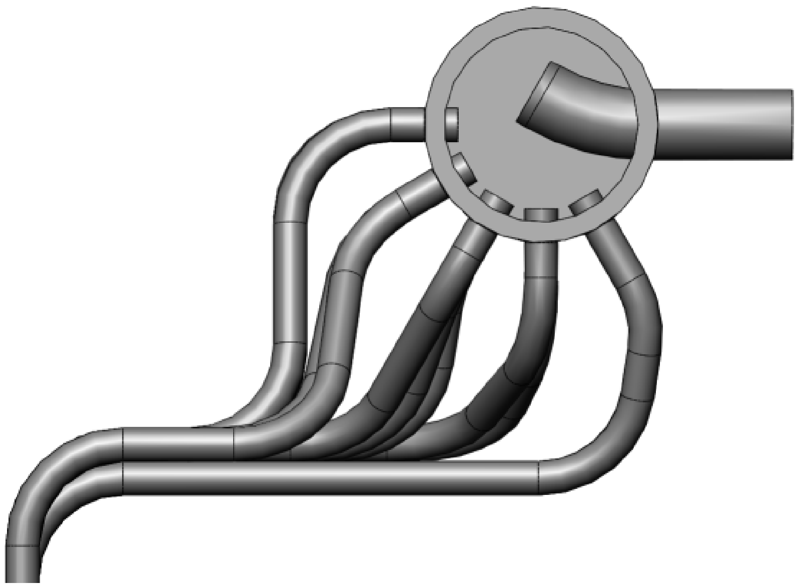

Back Panels (13 tubes)

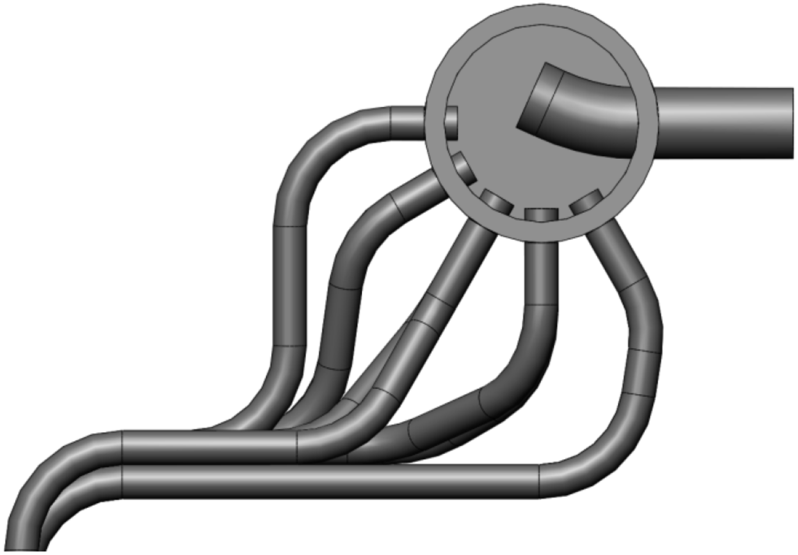

Fin Panels (9 tubes)

Header Modeling

- The average HTC over the entire zone was modeled across a range of temperatures and two flow directions for the two header types.
- Heat transfer coefficient contours on a center plane across a back header with an Air inlet flow rate of 15 g/s at 293 K and 250 kPa.